

Integrated Quantum-Walk Structure and NAND Tree on a Photonic Chip

Yao Wang^{1,2,*} Zi-Wei Cui^{3,4,*} Yong-Heng Lu,^{1,2} Xiao-Ming Zhang,⁵ Jun Gao,^{1,2}

Yi-Jun Chang,^{1,2} Man-Hong Yung^{3,4,6,7,†} and Xian-Min Jin^{1,2,3,4,‡}

¹Center for Integrated Quantum Information Technologies (IQIT), School of Physics and Astronomy and State Key Laboratory of Advanced Optical Communication Systems and Networks, Shanghai Jiao Tong University, Shanghai 200240, China

²CAS Center for Excellence and Synergetic Innovation Center in Quantum Information and Quantum Physics, University of Science and Technology of China, Hefei, Anhui 230026, China

³Department of Physics, Southern University of Science and Technology, Shenzhen 518055, China

⁴Shenzhen Institute for Quantum Science and Engineering, Southern University of Science and Technology, Shenzhen 518055, China

⁵Department of Physics, City University of Hong Kong, Tat Chee Avenue, Kowloon, Hong Kong SAR, China

⁶Guangdong Provincial Key Laboratory of Quantum Science and Engineering,

Southern University of Science and Technology, Shenzhen 518055, China

⁷Shenzhen Key Laboratory of Quantum Science and Engineering,

Southern University of Science and Technology, Shenzhen 518055, China



(Received 19 June 2020; accepted 8 September 2020; published 14 October 2020)

In the age of the post-Moore era, the next-generation computing model would be a hybrid architecture consisting of different physical components, such as photonic chips. In 2008, it was proposed that the solving of the NAND-tree problem can be sped up by quantum walk. This scheme is groundbreaking due to the universality of the NAND gate. However, experimental demonstration has not been achieved so far, mostly due to the challenge in preparing the propagating initial state. Here we propose an alternative solution by including a structure called a “quantum slide,” where a propagating Gaussian wave packet can be generated deterministically along a properly engineered chain. In our experimental demonstration, the optical NAND tree is capable of solving computational problems with a total of four input bits, based on the femtosecond laser 3D direct-writing technique on a photonic chip. These results remove one main roadblock to photonic NAND-tree computation, and the construction of a quantum slide may find other interesting applications in quantum information and quantum optics.

DOI: [10.1103/PhysRevLett.125.160502](https://doi.org/10.1103/PhysRevLett.125.160502)

Quantum walk, the quantum generalization of the classical random walk, is a natural platform for discovering exotic quantum phenomena and developing quantum algorithms [1–8]. Quantum-walk-based schemes have provided speed-up for various problems of particular interest, including Boson sampling [9–12], black-box problem [13], element distinctness [14], binary addition [15], factoring integers [16], and machine learning [17]. It has also been shown that quantum walk is powerful enough to perform universal quantum computation [18,19].

A NAND tree is a binary tree of NAND gates containing a total of N inputs but only one output, enabling the computation of arbitrary Boolean function of the form $F: \{0, 1\}^N \rightarrow \{0, 1\}$. While there are many classical algorithms for the NAND-tree problem [20,21], this task can be mapped to the quantum walk to speed up the computation. In 2008, Farhi *et al.* proposed a continuous quantum-walk-based protocol for balanced NAND tree for the first time [22]. Inspired by it, several discrete quantum-walk schemes have been developed [23,24]. The schemes have also been generalized to the unbalanced NAND formula [25–27], which can, in principle, represent arbitrary Boolean functions [28].

The original scheme of the NAND tree in Ref. [22] is based on a continuous quantum walk on a graph. As shown in Fig. 1, the graph contains a chain of uniformly coupled sites, called “runway,” the quantum NAND tree whose sites are connected in the structure as a binary tree, and a set of input nodes. Suppose the graph is represented by the adjacent matrix G , the time-independent Hamiltonian of the entire system is just $H = JG$, where J is the coupling constant. The input x is encoded by the on-off coupling of the input nodes (leaves) and the nodes on the top layer of the tree. For an incident wave packet with zero energy in the runway [22], if the computation outcome is $F(x) = 1$, the wave packet will pass through the quantum NAND tree; otherwise, the wave packet will be reflected when $F(x) = 0$. Therefore, by measuring whether the wave packet has passed through or been reflected, the binary computation outcome can be obtained.

The original protocol [22] of the quantum NAND tree is elegant and simple, and there is also proposal of realizing it on the molecular platform [29] being developed recently. However, its experimental realization remains challenging and, to our best knowledge, has not been

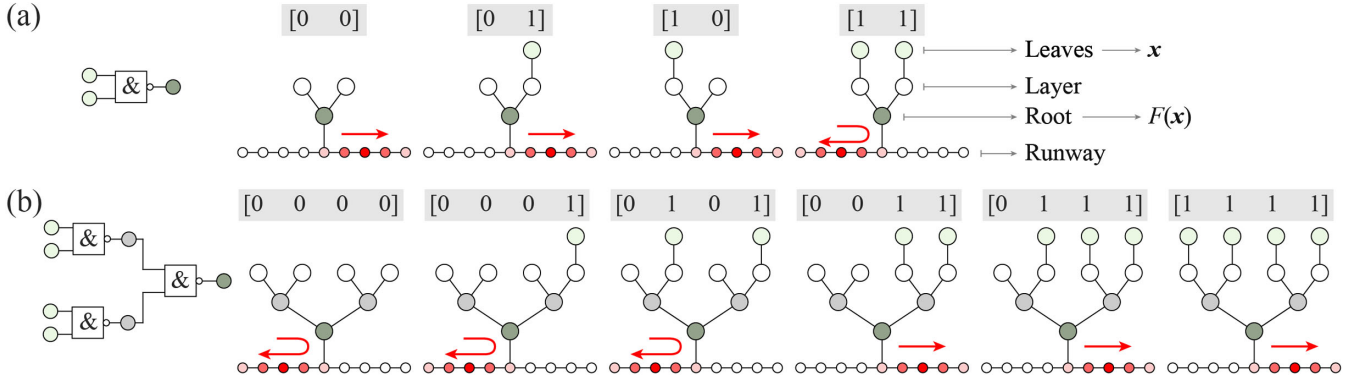


FIG. 1. Quantum NAND tree. The schematic of the tree structure with (a) one-layer branch and (b) two-layer branch. The site number in the last layer determines the number of input bits. The leaves on the last layer determine the input of the tree, if there is a leaf on the last layer, then the input of this site is one, and otherwise is zero. It is a NAND gate for each site on the layer besides the last layer. The logical value of the root presents the output result of the tree, which determines the evolution of the wave packet on the runway: the right-moving wave packet will back if the output result is zero, or go ahead if the output result is one.

successfully demonstrated yet. The major difficulty lies in the preparation of the initial state, where a truncated plane wave with sharp boundaries is required.

In this Letter, we propose an alternative approach by attaching a quantum slide (QS)—a chain with modulated adjacent coupling strength—to the runway. Consequently, a single photon (or even a light pulse) injected into a single site located at the edge of a QS, can naturally evolve through the quantum walk as a Gaussian wave packet along the runway.

We experimentally demonstrate this new approach on a photonic chip, where the associated graph structure is fabricated using the femtosecond laser direct-writing technique [30–33]. Our structure contains multiwaveguides with the number beyond 60, each of which corresponds to a node of the quantum walk. Instead of single photons, a light pulse is employed for preparing the Gaussian wave packet, which allows us to efficiently obtain the computational results by single-shot measurements. We first verify that the wave packet can be generated successfully by the QS, and transferred to the runway smoothly. Then, for both $N = 2$ and $N = 4$ cases, we measure the distribution of the photon intensity versus the evolution distance in the waveguide to verify the NAND-tree logic.

We first show how the Gaussian wave packet can be used for the NAND-tree logic computation and how QS can be employed for generating the Gaussian wave packet. For a runway with a total of L_{rw} sites labeled by s , the right-moving Gaussian wave packet is described by

$$|\psi_{\text{gs}}\rangle = A \sum_{s=1}^{L_{\text{rw}}} e^{-[(s-\mu)^2/4\sigma^2]} e^{-is(\pi/2)} |s\rangle, \quad (1)$$

where $\mu < L_{\text{rw}}/2$ is the center of the wave packet, A is the normalized coefficient as $A = (1/2\pi\sigma^2)^{1/4}$, where σ presents the standard deviation and is adopted here to characterize the wave packet width [34]. Note that the NAND tree is “planted” at the middle site, $s_{\text{mid}} = (L_{\text{rw}} + 1)/2$, of the runway.

Equation (1) can be regarded as the superposition of a set of plane waves whose eigenenergies are close to zero. Therefore, its evolution is similar to the ideal plane wave with zero energy as proposed in [22], and one can also obtain the computation outcome $F(\mathbf{x})$ by measuring whether the wave packet has passed through the NAND tree. More specifically, we define $P_+ = \sum_{s>s_{\text{mid}}} |s\rangle\langle s|$ as the projection on all the sites at the right of the middle site and assume σ increases quadratically with N ; i.e., $\sigma = \gamma\sqrt{N}$, where γ is a constant. The expectation value of P_+ after the wave packet passing through or being reflected by the quantum NAND tree satisfies (see Supplemental Material for theoretical analysis: quantum NAND tree [35])

$$\langle P_+ \rangle = F(\mathbf{x}) + O(\gamma^{-1/4}). \quad (2)$$

We also find that, to ensure good performance, L_{rw} should be proportional to σ . In particular, we numerically find that the optimum length is about $L_{\text{rw}} = 6\sigma$.

The Gaussian wave packet in Eq. (1) can be easily generated with a QS. For QS with L_{qs} sites, the coupling strength between the r th and $(r + 1)$ th site of the QS is set as $J_r = J\sqrt{r(2L_{\text{qs}} - 2 - r)/(L_{\text{qs}} - 1)}$, where J is the coupling strength at the runway. This type of structure is first introduced for perfect state transfer purpose [37,38]. Through quantum walk, a single excitation at site $r = 1$ can generate a stable Gaussian wave packet with high fidelity and transfer it to the runway. The width of the generated Gaussian wave packet is related to the site

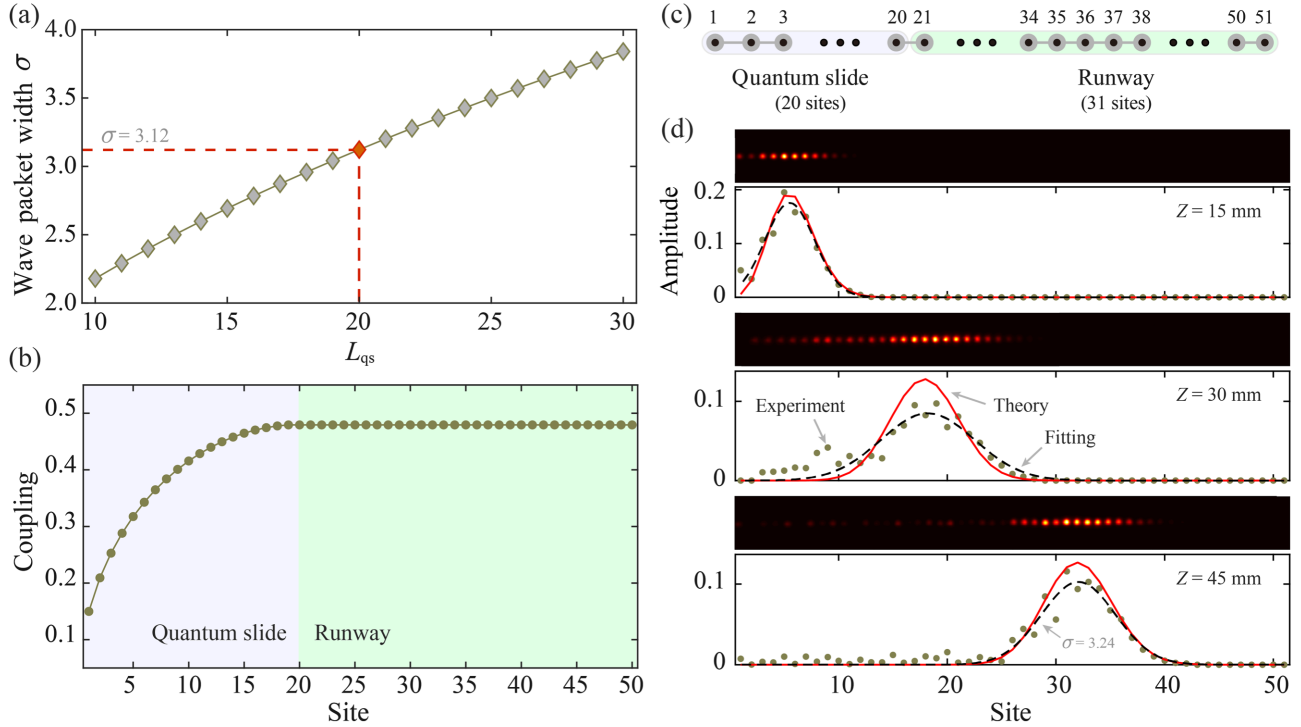


FIG. 2. Quantum slide. (a) The relationship between the wave packet width σ and the length of quantum slide L_{qs} . The red dashed line gives the parameter adopted in experiment. (b) The sketch of quantum slide. Twenty sites are designed for the QS; the wave packet obtained by the QS process transmits to the runway consisting of 31 sites. The sites in QS are labeled from 1 to 20, while the sites in runway are labeled from 21 to 51. (c) The distribution of the coupling strengths. (d) Measured output distribution of photons with different evolution distance in the QS process. The red lines are the theoretical results, the green points present the measured values, and the black dashed lines are the fitting result of the experimental values.

number of QS as shown in Fig. 2(a); more details about the theoretical analysis can be found in Supplemental Material for theoretical analysis: quantum slide [35].

As shown in Figs. 2(b) and 2(c), we set $L_{qs} = 20$ and $L_{rw} = 31$, respectively, in our experiment. For clarity, we relabel the s th site of the runway as the $(r + 20)$ th site. By coupling the last site in the quantum slide ($r = 20$) and the first site of the runway ($r = 21$) with coupling strength J , the generated Gaussian wave packet can be transferred to the runway smoothly. The structure accommodating the quantum-walk experiment is fabricated in borosilicate glass, and the coupling strength is experimentally measured to be $J = 0.48 \text{ mm}^{-1}$.

In Fig. 2(d), we show the measured photon distribution at evolution distance of 15, 30, and 45 mm. The results imply that the wave packet is successfully generated and transferred to the runway as expected, and the wave packet finally becomes stable and has a constant velocity in the runway. The measured velocity $v = 0.925 \pm 0.027 \text{ site/mm}^{-1}$ agrees well with the simulated result of $0.941 \text{ site/mm}^{-1}$ (see more discussion in the Supplemental Material for properties of the Gaussian wave-packet [35]).

The tree structure of the two-bit input NAND logical algorithm contains a one-layer branch, as shown in

Fig. 3(a), and the root site can exchange the photon with middle site of the runway labeled $r = 36$. The branch sites bridge the two sites of leaves with the root site, and the leaf site determines the input as one or zero. We fabricate four lattices with same parameters but different inputs $[0 \ 1]$, $[0 \ 0]$, $[1 \ 0]$, and $[1 \ 1]$. The photons with wavelength of 810 nm are transformed to pure horizontal polarization and then injected into the $r = 1$ site by a 30X objective lens. The output photon distribution is measured using a 10X objective lens and a CCD camera.

As discussed above, the NAND-tree structure determines whether the wave packet will pass the site $r = 36$ connecting the NAND tree. To quantify the result, we denote the sum of distribution probability over sites $21 \leq r \leq 35$ as S_L and the sum of distribution probability over the sites $37 \leq r \leq 51$ as S_R . In theoretical principle, we just need to simply compare the values of S_L and S_R to find whether the wave packet is reflected or transmitted by the tree. However, the photons will also occupy the sites in the tree in experiment, which is not presented in the theoretical analysis (see more discussion in the Supplemental Material for discussion on the experimental results [35]). We further set S_C as the sum of distribution probability over site in the NAND tree. According to the theory, the output result of

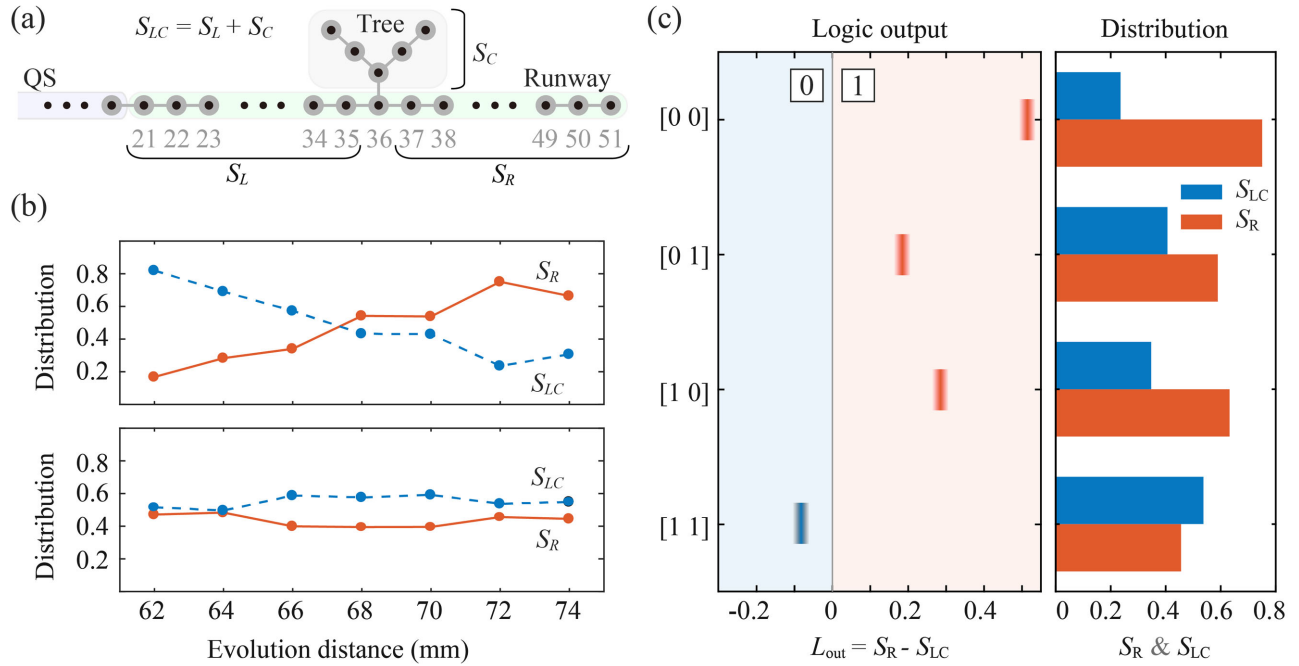


FIG. 3. Measured result of one-layer NAND tree. (a) The sketch of one-layer NAND-tree structure in experiment. S_L is the distribution amplitude summation of sites 21–35, S_R represents the distribution amplitude summation of sites 37–51, S_C is the distribution amplitude summation of sites in NAND-tree structure, and $S_{LC} = S_L + S_C$. (b) The evolution result of S_R and S_{LC} . For the case of input [0 0], the S_R goes larger than S_{LC} with the increase of evolution distance, representing that the wave packet goes pass the site connecting the tree, while the result is contrary for the case of input [1 1]. (c) The measured result of one-layer NAND tree. The logic output is determined by the L_{out} , which is obtained from the corresponding distributions of S_R and S_{LC} .

the NAND-tree logic value is one if $S_R > S_{LC}$, where $S_{LC} = S_L + S_C$, otherwise the logic output result is zero.

According to the measured output distributions, we recognize the intensity of each site and normalize the distribution with $S_R + S_{LC} = 1$. Taking the input [0 0] and [1 1], for example, we show the dynamical S_R and S_{LC} in Fig. 3(b); the S_R finally becomes larger than S_{LC} , representing that the wave packet goes past to the right side of the runway, and the corresponding result of the quantum NAND tree is one. It is contrary for the case of input [0 0], implying the logical result of zero. We define $L_{\text{out}} = S_R - S_{LC}$ as the quantum NAND-tree logical output; the logical value is zero if $L_{\text{out}} < 0$, otherwise, it is one. The measured NAND-tree logical output and detailed values of S_R and S_{LC} of all the cases at evolution distance of 72 mm are shown in Fig. 3(c). Our experimental results imply that the fabricated tree structures successfully realize the quantum NAND algorithm.

For the two-layer tree structure, there is four-bit input and the site number of the NAND tree varies from 7 to 11. As shown in Fig. 4, there are six types of logical inputs and we fabricate all of these types in a photonic chip. Taking the cases of input [0 0 0 0] and [0 1 0 1], the dynamical results of S_R and S_{LC} show the successful observation of logical output, implying that the evolution distance of 72 mm is appropriate for evaluating the

logical output of the quantum NAND tree. We measure the outgoing photon distributions at evolution distance of 72 mm and analyze the result of S_R , S_{LC} , and L_{out} . The results shown in Fig. 4 imply that the four-bit input quantum NAND algorithm is well realized and the visibility of the output result is stable. Different from the one-layer NAND tree, the two-layer NAND-tree structure is able to well control the passing or blocking on the wave packet in the runway in experiment. The reason behind may be that there are enough sites to influence the Hamiltonian of the whole lattice.

In conclusion, we present the first realization of quantum NAND-tree logic on an integrated photonic chip. We theoretically propose and experimentally realize a way of preparing a Gaussian wave packet with a quantum slide. Based on it, the NAND-tree logic is successfully demonstrated for the structure with up to $N = 4$ input. Compared to the molecular system [29], our platform has great advantages in integration and scalability. Moreover, the balanced tree structure in this Letter can be easily generalized to the unbalanced NAND formula, which can be applied to two-player games problems [28]. Finally, due to the universality of the NAND gate, it is possible to generalize the quantum NAND gate to represent arbitrary Boolean functions.

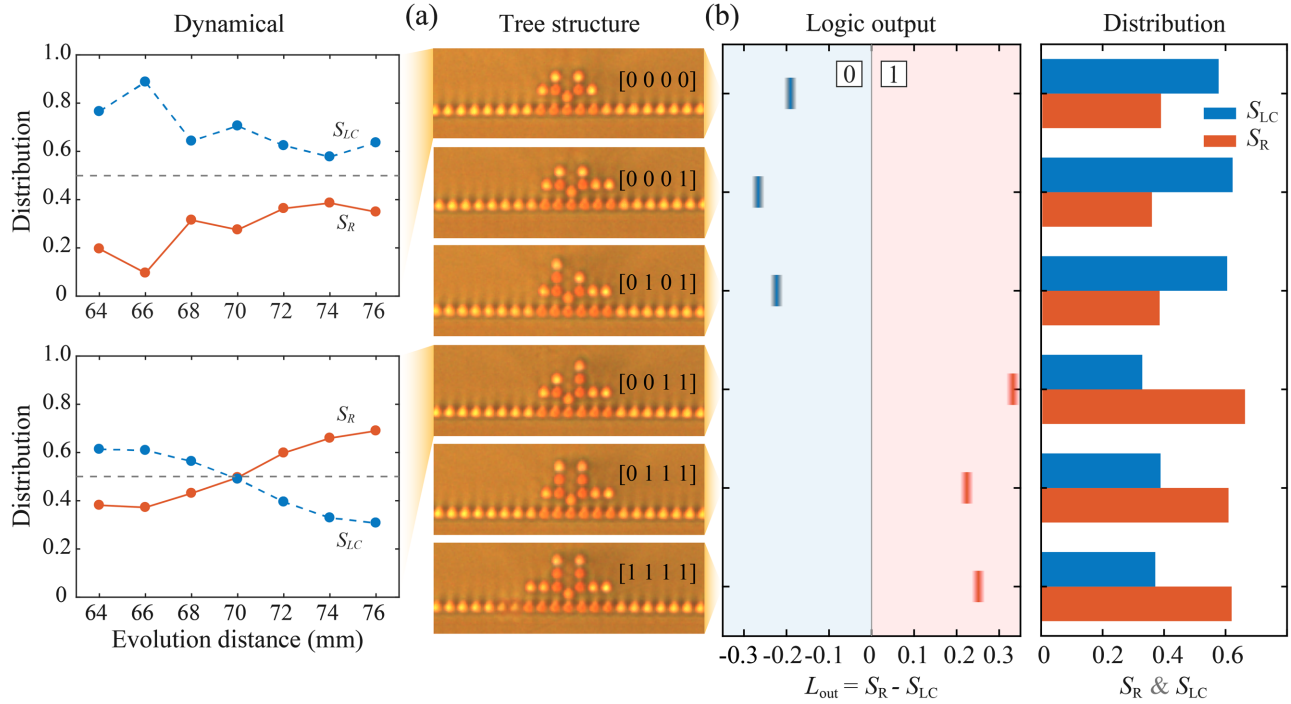


FIG. 4. Measured result of two-layer NAND tree. (a) The cross section micrograms of the NAND tree. There are six types of logical input for two-layer NAND tree. The insets show the dynamical result for the cases of input [0 0 0 0] and [0 0 1 1], respectively. For the case of input [0 1 0 1], the S_R goes larger than S_{LC} with the increase of evolution distance, representing that the wave packet goes past the site connecting the tree, while the result is contrary for the case of input [0 0 0 0]. (b) The measured logic output, S_R and S_{LC} of two-layer NAND tree. The four-bit input quantum NAND algorithm is well realized and the visibility of output result is stable.

The authors thank Jian-Wei Pan for helpful discussions. This research is supported by the Key-Area Research and Development Program of Guangdong Province (2018B030326001), the National Key R&D Program of China (2019YFA0308700, 2017YFA0303700), the National Natural Science Foundation of China (61734005, 11761141014, 11690033, 11875160, U1801661), the Science and Technology Commission of Shanghai Municipality (17JC1400403, 2019SHZDZX01), the Shanghai Municipal Education Commission (2017-01-07-00-02-E00049), the Natural Science Foundation of Guangdong Province (2017B030308003), Guangdong Provincial Key Laboratory (2019B121203002), the Science, Technology, and Innovation Commission of Shenzhen Municipality (JCYJ20170412152620376, JCYJ20170817105046702, KYTDPT20181011104202253), and the Economy, Trade, and Information Commission of Shenzhen Municipality (201901161512). X.-M. J. acknowledges support from Zhiyuan Innovative Research Center of Shanghai Jiao Tong University and additional support from a Shanghai talent program.

*These authors contributed equally to this work.

†yung@sustech.edu.cn

*xianmin.jin@sjtu.edu.cn

- [1] E. Farhi and S. Gutmann, Quantum computation and decision trees, *Phys. Rev. A* **58**, 915 (1998).
- [2] H. B. Perets, Y. Lahini, F. Pozzi, M. Sorel, R. Morandotti, and Y. Silberberg, Realization of Quantum Walks with Negligible Decoherence in Waveguide Lattices, *Phys. Rev. Lett.* **100**, 170506 (2008).
- [3] A. Peruzzo *et al.*, Quantum walks of correlated photons, *Science* **329**, 1500 (2010).
- [4] A. M. Childs and D. J. Strouse, Levinson's theorem for graphs, *J. Math. Phys. (N.Y.)* **52**, 082102 (2011).
- [5] A. M. Childs and D. Gosset, Levinson's theorem for graphs II, *J. Math. Phys. (N.Y.)* **53**, 102207 (2012).
- [6] A. Aspuru-Guzik and P. Walther, Photonic quantum simulators, *Nat. Phys.* **8**, 285 (2012).
- [7] H. Tang *et al.*, Experimental two-dimensional quantum walk on a photonic chip, *Sci. Adv.* **4**, eaat3174 (2018).
- [8] H. Tang *et al.*, Experimental quantum fast hitting on hexagonal graphs, *Nat. Photonics* **12**, 754 (2018).
- [9] M. A. Broome, A. Fedrizzi, S. Rahimi-Keshari, J. Dove, S. Aaronson, T. C. Ralph, and A. G. White, Photonic boson sampling in a tunable circuit, *Science* **339**, 794 (2013).
- [10] J. B. Spring *et al.*, Boson sampling on a photonic chip, *Science* **339**, 798 (2013).
- [11] M. Tillmann, B. Dakić, R. Heilmann, S. Nolte, A. Szameit, and P. Walther, Experimental boson sampling, *Nat. Photonics* **7**, 540 (2013).
- [12] A. Crespi *et al.*, Integrated multimode interferometers with arbitrary designs for photonic boson sampling, *Nat. Photonics* **7**, 545 (2013).

- [13] A. M. Childs, R. Cleve, E. Deotto, E. Farhi, S. Gutmann, and D. A. Spielman, in *Proceedings of the Thirty-Fifth Annual ACM Symposium on Theory of Computing* (ACM, San Diego, CA, 2003), pp. 59–68.
- [14] A. Ambainis, Quantum walk algorithm for element distinctness, *SIAM J. Comput.* **37**, 210 (2007).
- [15] D. Deutsch and R. Jozsa, Rapid solution of problems by quantum computation, *Proc. R. Soc. A* **439**, 553 (1992).
- [16] P. W. Shor, Polynomial-time algorithms for prime factorization and discrete logarithms on a quantum computer, *SIAM J. Comput.* **26**, 1484 (1997).
- [17] G. D. Paparo, V. Dunjko, A. Makmal, M. A. Martin-Delgado, and H. J. Briegel, Quantum Speedup for Active Learning Agents, *Phys. Rev. X* **4**, 031002 (2014).
- [18] A. M. Childs, Universal Computation by Quantum Walk, *Phys. Rev. Lett.* **102**, 180501 (2009).
- [19] A. M. Childs, D. Gosset, and Z. Webb, Universal computation by multiparticle quantum walk, *Science* **339**, 791 (2013).
- [20] M. E. Saks and A. Wigderson, Probabilistic Boolean decision trees and the complexity of evaluating game trees, *IEEE Symp. Found. Comput. Sci.* **27**, 29 (1986).
- [21] M. Santha, On the Monte carlo boolean decision tree complexity of read-once formulae, *Random Struct. Algorithms* **6**, 75 (1995).
- [22] E. Farhi, J. Goldstone, and S. Gutmann, A quantum algorithm for the Hamiltonian NAND tree, *Theory Comput.* **4**, 169 (2008).
- [23] A. Ambainis, A nearly optimal discrete query quantum algorithm for evaluating NAND formulas, [arXiv:0704.3628](https://arxiv.org/abs/0704.3628).
- [24] A. M. Childs, R. Cleve, S. p. Jordan, and D. Yonge-Mallo, Discrete-query quantum algorithm for NAND trees, *Theory Comput.* **5**, 119 (2009).
- [25] A. M. Childs, B. W. Reichardt, R. Spalek, and S. Zhang, Every NAND formula of size N can be evaluated in time $N^{1/2+o(1)}$ on a quantum computer, [arXiv:0703015](https://arxiv.org/abs/0703015).
- [26] A. Ambainis, A. M. Childs, B. W. Reichardt, R. Spalek, and S. Zhang, Any AND-OR formula of size N can be evaluated in time $N^{1/2+o(1)}$ on a quantum computer, *SIAM J. Comput.* **39**, 2513 (2010).
- [27] R. Cleve, D. Gavinsky, and D. L. Yonge-Mallo, Quantum algorithms for evaluating min-max trees, in *Workshop on Quantum Computation, Communication, and Cryptography* (Springer, Berlin, Heidelberg, 2008), pp. 11–15.
- [28] B. w. Reichardt, Faster quantum algorithm for evaluating game trees, in *Proceedings of the Twenty-Second Annual ACM-SIAM Symposium on Discrete Algorithms* (Society for Industrial and Applied Mathematics, 2011), pp. 546–559 [[arXiv:0907.1623](https://arxiv.org/abs/0907.1623)].
- [29] P. W. K. Jensen, C. Jin, P.-L. Dallaire-Demers, A. Aspuru-Guzik, and G. C. Solomon, Molecular realization of a quantum NAND tree, *Quantum Sci. Technol.* **4**, 015013 (2018).
- [30] K. M. Davis, K. Miura, N. Sugimoto, and K. Hirao, Writing waveguides in glass with a femtosecond laser, *Opt. Lett.* **21**, 1729 (1996).
- [31] A. Szameit, F. Dreisow, T. Pertsch, S. Nolte, and A. Tünnermann, Control of directional evanescent coupling in fs laser written waveguides, *Opt. Express* **15**, 1579 (2007).
- [32] Z. Chaboyer, T. Meany, L. G. Helt, M. J. Withford, and M. J. Steel, Tunable quantum interference in a 3D integrated circuit, *Sci. Rep.* **5**, 9601 (2015).
- [33] Y. Wang *et al.*, Parity-Induced Thermalization Gap in Disordered Ring Lattices, *Phys. Rev. Lett.* **122**, 013903 (2019).
- [34] The full width at half maximum of the Guassion wave packet is proportional to the standard deviation as $2\sqrt{2\ln 2}\sigma$, which allows the σ to characterize the wave packet width.
- [35] See Supplemental Material at <http://link.aps.org/supplemental/10.1103/PhysRevLett.125.160502> for details, which includes Ref. [36].
- [36] R. Keil, B. Pressl, R. Heilmann, M. Grfe, G. Weihs, and A. Szameit, Direct measurement of second-order coupling in a waveguide lattice, *Appl. Phys. Lett.* **107**, 241104 (2015).
- [37] M. Christandl, N. Datta, A. Ekert, and A. J. Landahl, Perfect State Transfer in Quantum Spin Networks, *Phys. Rev. Lett.* **92**, 187902 (2004).
- [38] M. B. Plenio, J. Hartley, and J. Eisert, Dynamics and manipulation of entanglement in coupled harmonic systems with many degrees of freedom, *New J. Phys.* **6**, 36 (2004).